9-1-2023

Keck spectroscopy of NGC 1052-DF9: stellar populations in the context of the NGC 1052 group

Jonah S. Gannon
Swinburne University of Technology

Maria Luisa Buzzo
Swinburne University of Technology

Anna Ferre-Mateu
Instituto Astrofisico de Canarias

Duncan A. Forbes
Swinburne University of Technology

Jean P. Brodie
Swinburne University of Technology

See next page for additional authors

Recommended Citation

Authors

Jonah S. Gannon, Maria Luisa Buzzo, Anna Ferre-Mateu, Duncan A. Forbes, Jean P. Brodie, and Aaron J. Romanowsky

Keck spectroscopy of NGC 1052-DF9: stellar populations in the context of the NGC 1052 group

Jonah S. Gannon [1,2]★ Maria Luisa Buzzo [1,2] Anna Ferré-Mateu [3,4] Duncan A. Forbes,[1,2] Jean P. Brodie[1,2,5] and Aaron J. Romanowsky [5,6]

[1]*Centre for Astrophysics and Supercomputing, Swinburne University, John Street, Hawthorn, VIC 3122, Australia*
[2]*ARC Centre of Excellence for All Sky Astrophysics in 3 Dimensions (ASTRO 3D), Australia*
[3]*Instituto de Astrofísica de Canarias, Calle Vía Láctea S/N, E-38205 La Laguna, Tenerife, Spain*
[4]*Departamento de Astrofísica, Universidad de La Laguna, E-38206 La Laguna (S.C. Tenerife), Spain*
[5]*Department of Astronomy & Astrophysics, University of California Santa Cruz, 1156 High Street, Santa Cruz, CA 95064, USA*
[6]*Department of Physics and Astronomy, San José State University, One Washington Square, San Jose, CA 95192, USA*

ABSTRACT

In this study, we use Keck/Keck Cosmic Web Imager spectroscopy to measure the age, metallicity, and recessional velocity of NGC 1052-DF9 (DF9), a dwarf galaxy in the NGC 1052 group. We compare these properties to those of two other galaxies in the group, NGC 1052-DF2 and NGC 1052-DF4, which have low dark matter content. The three galaxies are proposed constituents of a trail of galaxies recently hypothesized to have formed as part of a 'bullet dwarf' collision. We show that the ages and total metallicities of the three galaxies are within uncertainties of one another which may be expected if they share a related formation pathway. However, the recessional velocity we recover for DF9 ($1680 \pm 10 \, \mathrm{km \, s^{-1}}$) is higher than predicted for a linearly projected interpretation of the 'bullet dwarf' trail. DF9 is then either not part of the trail or the correlation of galaxy velocities along the trail is not linear in 2D projection due to their 3D geometry. After examining other proposed formation pathways for the galaxies, none provide a wholly satisfactory explanation for all of their known properties. We conclude further work is required to understand the formation of this interesting group of galaxies.

Key words: galaxies: dwarf – galaxies: formation – galaxies: fundamental parameters – galaxies: nuclei.

1 INTRODUCTION

The galaxies NGC 1052-DF2 (hereafter DF2)[1] and NGC 1052-DF4 (hereafter DF4)[2] in the NGC 1052 group have been highly controversial due to claims of their dark matter deficient nature (van Dokkum et al. 2018a, 2019; Danieli et al. 2019) and their overluminous globular cluster (GC) populations (van Dokkum et al. 2018a, 2019; Shen, van Dokkum & Danieli 2021a). Many attempts have been made to describe the formation of each galaxy individually, not considering these galaxies may be related. These include tidal stripping from a massive object (Ogiya 2018; Montes et al. 2020; Nusser 2020; Jackson et al. 2021; Macciò et al. 2021; Moreno et al. 2022; Ogiya, van den Bosch & Burkert 2022), their formation as tidal dwarf galaxies from stripped H I gas (van Dokkum et al. 2018a; Fensch et al. 2019a), or as the result of extreme interstellar medium conditions from e.g. a high-redshift merger (Trujillo-Gomez et al. 2021). If the formation pathway of these two galaxies is a rare occurrence, it would be an unlikely coincidence to find two in the same galaxy group (although

see Moreno et al. 2022). Furthermore, some of these formation scenarios (e.g. tidal stripping) do not explain the population of overluminous GCs around each galaxy (Shen et al. 2021a).

In a separate scenario, the formation of DF2, DF4, and up to nine other galaxies in the NGC 1052 group may be the result of a high-speed galaxy collision (Silk 2019; Shin et al. 2020; Lee, Shin & Kim 2021; van Dokkum et al. 2022a). Briefly, van Dokkum et al. (2022a, hereafter vD + 22) identified a near-linear 'trail' of galaxies in projection and suggested these may be the result of a high-speed galaxy collision ∼8 Gyr ago. This collision separates off the existing stars, GCs, and dark matter from the gas, which later collapses to form new galaxies and GCs. Such a scenario then leaves the two progenitor galaxies dark matter dominated and stripped of gas at either end of a trail of newly formed dark matter-free galaxies (see further in extended Fig. 1; vD + 22). They dubbed this proposal the 'bullet dwarf' scenario due to similarities with a miniaturized version of the bullet cluster.

Key predictions from the 'bullet dwarf' scenario are that the newly formed galaxies and their constituents (e.g. GCs) should have:

(i) Similar ages and metallicities due to their formation from the same stripped gas.

(ii) Recessional velocities that are correlated with their on-sky position. However, we note that this correlation is not expected to

★ E-mail: jonah.gannon@gmail.com
[1]DF2 was first discovered by Fosbury et al. (1978) although it was not named until more recently (Karachentsev et al. 2000).
[2]For a full summary of additional designations for both DF2 and DF4, see table 1 of Román, Castilla & Pascual-Granado (2021b).
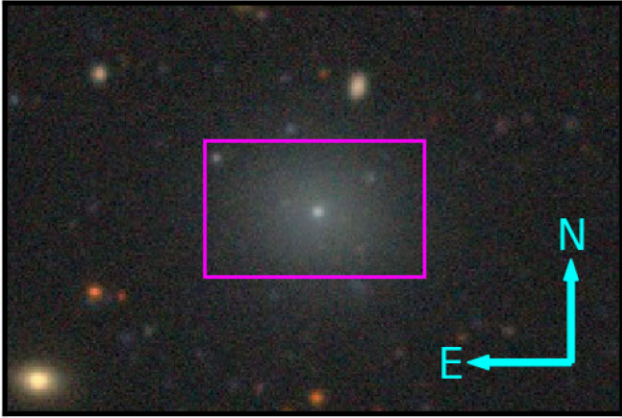
Figure 1. A 90 arcsec × 60 arcsec (8.4 kpc × 5.6 kpc at NGC 1052 distance) DECaLS cutout centred on DF9. The magenta rectangle indicates the field of view of our KCWI observations. North and east are as indicated (cyan arrows). We identify the central compact source as the nucleus of DF9.

be linear in 2D projection for most 3D geometries in the system (vD + 22).

(iii) An extreme lack of dark matter, reflective of their formation from gas stripped from a dark matter halo.

The trail galaxies DF2 and DF4 have already been tested for each of these three requirements. Both have been found to be dark matter deficient (van Dokkum et al. 2018a, 2019; Danieli et al. 2019; Emsellem et al. 2019; Montes et al. 2020; Keim et al. 2022). Additionally, DF2 and DF4 have had their stellar population parameters (i.e. age and metallicity) measured from either spectroscopy (DF2; Fensch et al. 2019a; Ruiz-Lara et al. 2019) or spectral energy distribution (SED) fitting (DF2/DF4; Buzzo et al. 2022). The ages and metallicities for both galaxies are within uncertainties of one another (Buzzo et al. 2022). Finally, both DF2 and DF4 have measured recessional velocities (Danieli et al. 2019; van Dokkum et al. 2019) that place initial constraints on the geometry of the collision (vD + 22).

In this work, we study the next brightest galaxy located along this bullet trail, NGC 1052-DF9 (hereafter DF9). After DF2 and DF4, DF9 is the only galaxy remaining on the trail bright enough to be observable with current spectrographs in reasonable integration times. We note that DF9 was excluded by vD + 22 as a member of the objectively selected trail as it was not in the catalogue of Román et al. (2021b) due to its relative brightness. However, vD + 22 still noted it may be a trail member. It is also one of only two other galaxies on the trail that has a GC system and is nucleated (Buzzo et al. 2023). It is therefore an important test of the bullet trail hypothesis. Throughout this work, we assume a distance to DF9 of 20 Mpc ($m - M = 31.5$) that is the same distance assumed in the related work of Buzzo et al. (2023) along with the published works of van Dokkum et al. (2018b) and Shen et al. (2021a), which concern DF2/DF4. We note that there has been some controversy about this assumed distance to these dwarf galaxies (see e.g. Trujillo et al. 2019), but recent deep *Hubble Space Telescope* imaging supports our assumption (Shen et al. 2021b). Magnitudes are in the AB system.

2 KECK COSMIC WEB IMAGER DATA

The Keck Cosmic Web Imager (KCWI) data used in this work were observed on the night of 2022 January 29 as part of programme N195 (PI: Romanowsky). Conditions were clear with 0.9 arcsec seeing in which a single 1200 s exposure was observed. The data were observed

Table 1. The basic properties of NCG 1052-DF9. From top to bottom, the entries are (1) Right ascension (J2000), (2) Declination (J2000), (3) g-band apparent magnitude (m_g), (4) total stellar mass ($M_\star$), (5) central g-band surface brightness [$\mu_g(0)$], (6) half-light radius in arcsec, (7) half-light radius in kpc at the assumed 20 Mpc distance (R_e), (8) recessional velocity (V_r) with PPXF given uncertainty, and (9) assumed distance. All values except the stellar mass, recessional velocity, and half-light radius at our assumed distance are taken from Trujillo et al. (2021).

RA (J2000)	02:40:07.01
Dec. (J2000)	−08:13:44.4
m_g (mag)	17.17
$M_\star$ (M$_\odot$)	1.31×10^8
$\mu_g(0)$ (mag arcsec^{-2})	23.81
R_e (arcsec)	11.1
R_e (kpc)	1.08
V_r (km s^{-1})	1680 (10)
D (Mpc)	20

using the large slicer with the BL grating and cover a wavelength range of 3554–5574 Å.th A spectral resolution of $R = 785$ ($\sigma_{Inst} = 160$ km s^{-1}) at 4500 Å was measured on the calibration arc files. This resolution was degraded from expected instrument performance due to software errors during instrument configuration.

These data were reduced using the standard KCWI data reduction pipeline (Morrissey et al. 2018) and were subsequently cropped per Gannon et al. (2020). Two spectra were extracted from the resulting data cube: (1) a spectrum of the nucleus and (2) a galaxy spectrum excluding the central nucleus. The nucleus spectrum was extracted using a 4 spaxel × 1 spaxel (1.17 arcsec × 1.35 arcsec) box with the remainder of the slicer, excluding a 1 spaxel buffer around the extraction box, as background (i.e. both sky and galaxy). It has a final signal-to-noise ratio of 13 Å^{-1}. The galaxy spectrum was extracted using a 41 spaxel × 13 spaxel (11.95 arcsec × 17.65 arcsec) box with the outskirts of the data cube as background. Two compact sources, including the nucleus, were removed from both the galaxy and background regions. It has a final signal-to-noise ratio of 14 Å^{-1}. We display a DECaLS stamp centred on DF9 (https://www.legacysurvey.org/viewer), along with KCWI pointing, in Fig. 1.

3 LITERATURE DATA FOR DF9

We note that DF9 was also presented in Trujillo et al. (2021) as SDSS J024007.01–081344.4. From their deep imaging, we take the right ascension, declination, apparent g-band magnitude, central g-band surface brightness, and g-band half-light radius. We list these in Table 1. We note that, based on their measured half-light radius and central surface brightness, DF9 is both too bright and too small to be considered an 'ultra-diffuse galaxy' using the definition of van Dokkum et al. (2015).

We additionally note the central compact object in DF9 that was identified as a possible nucleus from Buzzo et al. (2023). They reported an apparent magnitude of $m_g = 21.9$ mag ($M_g = -9.6$ mag) and noted it has colours consistent with those of a GC ($\langle g - i \rangle = 0.71$ and $\langle u - i \rangle = 1.68$). This is despite it being quite luminous for a 'normal' GC.

4 STELLAR POPULATION RESULTS

To extract stellar population parameters (i.e. mean mass-weighted ages and metallicities), we fit each spectrum with PPXF (Cappellari
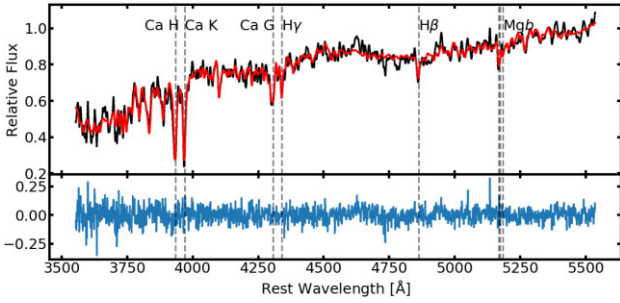
Figure 2. A Gaussian smoothed ($\sigma = 1$ Å) KCWI spectrum for DF9's stellar body (black; spectrum 2 in text) with example PPXF fit (red) displayed at the rest wavelengths. Residuals from the non-smoothed fit are shown at the bottom (blue). The prominent hydrogen, calcium, and magnesium absorption features are indicated by dashed vertical lines.

Table 2. A comparison of the stellar population properties derived in this work for DF9 to those for DF2 and DF4 from the literature. From left to right the columns are (1) the data used to derive the stellar populations, (2) the target galaxy, (3) [Z/H] metallicity, (4) age in Gyr, and (5) the source for the data. Where relevant, uncertainties are given in parentheses. The values quoted for DF9 are for a spectrum that does not include the nucleus. The row for DF2 listed as being the 'mean' presents the error-weighted average of three studies on DF2. RL19 refers to Ruiz-Lara et al. (2019). F19 refers to Fensch et al. (2019a). B22 refers to Buzzo et al. (2022).

Data	Object	[Z/H] (dex)	Age (Gyr)	Source
Spectrum	DF9	$-1.00\,(^{+0.04}_{-0.09})$	$9.79\,(^{+0.48}_{-0.6})$	This work
Spectrum	DF9 nucleus	$-1.07\,(^{+0.03}_{-0.04})$	$8.72\,(^{+0.57}_{-1.16})$	This work
Spectrum	DF2	$-1.20\,(0.07)$	$9.8\,(0.5)$	RL19
Spectrum	DF2	$-1.07\,(0.12)$	$8.9\,(1.5)$	F19
Spectrum	DF2 GCs	$-1.63\,(0.09)$	$8.9\,(1.8)$	F19
SED	DF2	$-1.11\,(^{+0.35}_{-0.28})$	$7.97\,(^{+1.83}_{-2.73})$	B22
Mean	DF2	$-1.14\,(0.12)$	$9.4\,(0.9)$	This work
SED	DF4	$-1.08\,(^{+0.35}_{-0.22})$	$8.76\,(^{+2.91}_{-1.51})$	B22

5 DISCUSSION

5.1 Formation of the nucleus

In Fahrion et al. (2022, fig. 6 and Fahrion et al. 2020, 2021 therein), a transition is seen between galaxies with nuclear star clusters forming via GC mergers and *in situ* nuclear star cluster formation. Based on the stellar mass of DF9 and its nucleus, we expect it to reside in the regime where other galaxies are known to mostly have nuclei forming via GC mergers. However, the nucleus has approximately seven times the average mass of a Milky Way GC ($\sim 2\,M_\odot \times 10^5$ $M_\odot$; Harris 1996; 2010 version), suggesting a moderate number of GCs would be required if it were to form via GC mergers. This is at a slight tension with the relatively sparse GC system observed at present times (~ 3 GCs; Buzzo et al. 2023), as it would require a large fraction of its historical GC system to have merged into the nucleus.

Furthermore, in the *top panel* of Fig. 3 we show the star formation histories of DF9 and its nucleus. These star formation histories are not regularized, but our conclusions do not change under reasonable regularization choices. Given their similar profiles, it seems quite likely that the nucleus formed at a similar epoch to the galaxy. This is further supported by the common metallicities between the two components suggesting that both formed from similarly enriched gas. This is not as expected in the GC merger formation scenario where the nucleus tends to be older and more metal-poor than the surrounding galaxy. It seems therefore likely that some combination of *in situ* formation and GC mergers took place in the formation of the nucleus of DF9.

5.2 Formation of DF9

In Fig. 3, *lower left*, we show the ages and metallicities we have derived for DF9 in comparison to results from the literature for DF2's stellar body, DF2's GC system, and DF4's stellar body (Fensch et al. 2019a; Ruiz-Lara et al. 2019; Buzzo et al. 2022). For DF2, we plot the error-weighted average of the three age/metallicity measurements from Fensch et al. (2019a), Ruiz-Lara et al. (2019), and Buzzo et al. (2022) so as not to crowd the plot. We find that the ages and metallicities of the three galaxies (i.e. DF2, DF4, and DF9) are within uncertainties of one another.

Despite the similar stellar populations, there exists the possibility that the three galaxies have unrelated formation pathways. In Fig. 3,
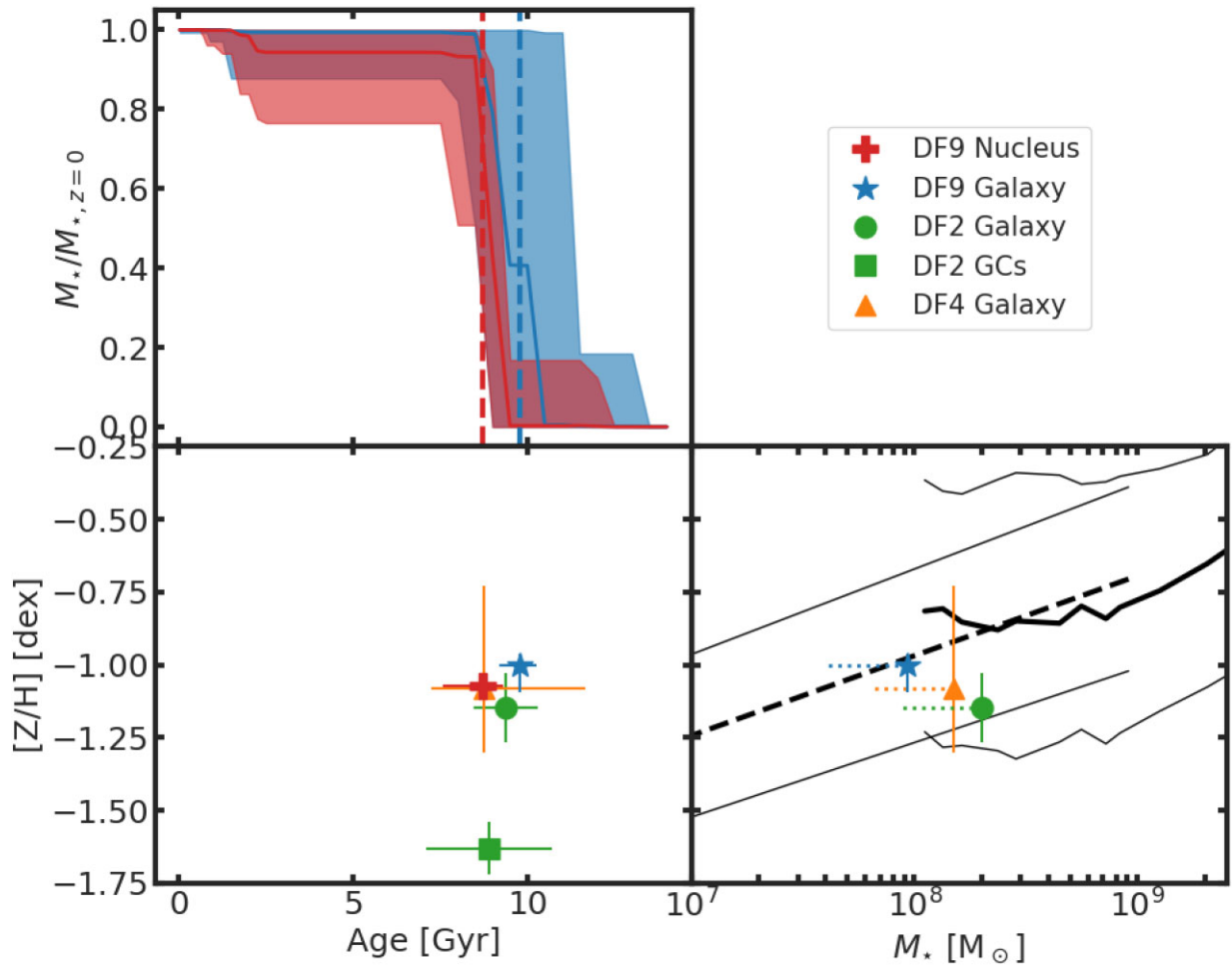
2017) and the MILES stellar library (Vazdekis et al. 2015). We use MILES simple stellar population models assuming a Kroupa initial mass function (Kroupa 2001) and BaSTI isochrones. These models have total metallicities ranging from [Z/H] $= -2.42$ to $+ 0.4$ dex and ages ranging from 0.03 to 14 Gyr. The version of these models used assumes solar-scaled abundances (i.e. MILES BaseFe).

The recessional velocity of DF9 was measured from a single fit with an additional eighth-order additive and multiplicative polynomial. From this fit, we measure a recessional velocity of 1680 ± 10 km s^{-1} after barycentric correction (Tollerud 2015). The uncertainty on the recessional velocity is that given by PPXF; however, we note it will not include uncertainty in our wavelength calibration which is likely ~ 40 km s^{-1}. Our recessional velocity corrects the erroneous listing of DF9 as being a $z = 0.933$ quasar from SDSS.

We then proceeded to measure the age and metallicity of DF9. These were measured as the median values of 256 fits resulting from all combinations of including a 0–15 degree additive and a 0–15 degree additive polynomial in the fitting procedure. Additive and multiplicative polynomials correct for continuum shape errors that may be introduced during flux calibration. Fig. 2 shows an example of one such PPXF fit to the spectrum of DF9's stellar body (spectrum 2). Uncertainties are taken from the 14th and 86th percentiles of the resulting parameter distributions. Our final results using this method for the mean mass-weighted age and metallicity of both spectra we extract are shown in Table 2.

We checked for the effect of using the non-alpha-enhanced MILES models by refitting the data with the alpha-enhanced MILES model (i.e. [α/Fe] $= 0.4$ dex). The usage of alpha-enhanced models results in metallicities that are on an average 0.2 dex more metal-rich and 0.57 Gyr older than the values quoted in Table 2. We choose, however, to quote values for the non-alpha enhanced models as these represent the best match to the methods used in Fensch et al. (2019a) for DF2, which we use for comparison in Section 5. We note all of our PPXF fitting does not apply regularization to the output template weighting. Doing so will result in slightly younger ages (~ 1 Gyr depending on the choice of value).

Based on our fitting of DF9, we measure a mass-to-light ratio in g band of 2.2 which implies a total stellar mass for the galaxy of $1.31\,M_\odot \times 10^8\,M_\odot$. We include this value in Table 1. This stellar mass is approximately that of DF4 and only slightly less than that of DF2. Based on our fitting of its nucleus alone, we measure a mass-to-light ratio in g band of 1.9, which implies a total stellar for the nucleus of $1.46\,M_\odot \times 10^6\,M_\odot$. Mass-to-light ratios assume the same Kroupa (2001) initial mass function as our stellar library.

Figure 3. A comparison of our derived stellar population parameters of DF9 and its nucleus to measurements for DF2 and DF4. Top panel: PPXF derived, non-regularized star formation histories for both DF9 (blue) and its nucleus (red). Solid lines indicate the mean relation with shading between the earliest and latest star formation histories derived in our fitting. Vertical lines represent the mass-weighted ages of each. The star formation histories are consistent with both the nucleus and the galaxy forming at the same time. This conclusion will not change under reasonable regularization choices. Bottom left: Mass-weighted age versus metallicity. We show our values for DF9's nucleus (red plus) and for the stellar body without the nucleus (blue star). These are compared to: the mean age and metallicity of the stellar body of DF2 from Fensch et al. (2019a), Ruiz-Lara et al. (2019), and Buzzo et al. (2022, green circle); the GCs around DF2 from Fensch et al. (2019a, green square) and DF4's stellar body from Buzzo et al. (2022, orange triangle). The ages and metallicities of DF2, DF4, and DF9 are within uncertainties of one another but DF2's GC system is significantly more metal-poor. Bottom right: Metallicity versus stellar mass. Plotted points for the galaxies' stellar bodies are the same as in the previous panel. Mass–metallicity relationships are included based on Panter et al. (2008) and Simon (2019). The dotted lines indicate the expected change in stellar mass if the galaxies are at the closer claimed distance (Trujillo et al. 2019). All three galaxies are within the scatter of established mass–metallicity relations.

lower right, we show DF2, DF4, and DF9 in stellar mass–metallicity space. We include the established relationships of Panter et al. (2008) and Simon (2019). We note all of DF2/DF4/DF9 lie within the scatter of the mass–metallicity relationship. The common metallicities of the three galaxies may therefore simply be a consequence of the known mass–metallicity relationship. Therefore, we cannot be conclusive that the formation of these galaxies must be related, and that their similar stellar population properties are not the result of random chance. Despite this, for the remainder of the discussion, we will assume a common formation pathway for all three galaxies.

5.3 The bullet trail

Having the ages and metallicities of DF2/DF4/DF9 within uncertainties of one another is as expected if they formed in the 'bullet dwarf' formation scenario of vD + 22. However, we show that in Fig. 3,

lower left, the GC system of DF2 is on average more metal-poor than its stellar body (Fensch et al. 2019a). Furthermore, given the similar colours of DF2's and DF4's GC systems and how the stellar bodies of both galaxies are on average redder than their GC systems (van Dokkum et al. 2022b), it seems likely DF4's GC system may also be more metal-poor than its stellar body.

In the context of the bullet scenario, it is not clear how the galaxy and its GC system could have differing metallicity if they both form in a burst of high-pressure star formation from the same gas (which is needed to explain the overluminous GCs). Further star formation would be required to enrich the mass-weighted metallicity of the galaxy with respect to its GCs. However, this star formation would also be required to not have a large effect on the mass-weighted age that is measured to be within uncertainties of the age of the GCs. Further modelling of the post-collision metallicity enrichment of the galaxies is needed to understand this dilemma.

A separate source for confirmation of this bullet trail hypothesis would come from the recessional velocity of DF9. We calculate DF9 to be 14.3 arcmin west of NGC 1052. Using the relation $cz = 1700 - 10\,\Delta$RA from vD + 22, we predict a recessional velocity of $1557\,\mathrm{km\,s^{-1}}$ for DF9. This is $123\,\mathrm{km\,s^{-1}}$ (or $\sim 12 \times$ our uncertainty) lower than our measured recessional velocity (i.e. $1680\,\mathrm{km\,s^{-1}}$). vD + 22 noted that this relationship is expected to have considerable scatter and that the predicted recessional velocities based on galaxies' 2D projected positions may not be linearly increasing for most geometries once calculated in 3D. We suggest that, even in the case of considerable scatter, DF9 would not follow this relationship if it were linear as calculated. In order for the bullet formation scenario to be valid and cause the formation of DF9, the 3D geometry of the bullet trail must be such that the relationship is non-linear once projected into 2D.

5.4 Tidal debris

These galaxies may all have formed as tidal dwarf galaxies from gas stripped during a galaxy interaction, representing a more gentle case of the above 'bullet dwarf' formation scenario. The common ages and metallicities are then also evidence for this tidal formation. Evidence from other systems suggests that galaxies of similar R_e, stellar mass and low surface brightness to DF2/DF4/DF9 can form as tidal debris as they are embedded in tidal debris filaments (see e.g. Román et al. 2021a or Iodice et al. 2021).

We note that DF2 is not detected in deep H I imaging (Sardone et al. 2019) and there are no convincing H I structures associated with any of DF2/DF4/DF9 (Müller et al. 2019). Were these galaxies to form from tidally stripped H I gas, they must have now depleted their gas reservoir below the detection limits of these surveys. This is possible for these galaxies given their intermediate/old ages. However, in this generalized tidal debris scenario, it is difficult to explain the anomalous GC systems found for both DF2 and DF4 (Shen et al. 2021a). For example, simulations of GC mergers based on the known observations of DF2 and DF4 demonstrate that these are not able to explain the overluminous GC systems (Dutta Chowdhury, van den Bosch & van Dokkum 2020). An additional special mechanism would therefore be required to induce the formation of the overluminous GCs.

In addition to these problems, tidal dwarf galaxies are known to exhibit high metallicities for their stellar masses owing to their formation from enriched material (see e.g. Sales et al. 2020 or Román et al. 2021a). All of our galaxies follow the established mass–metallicity relationship and thus do not have the high metallicities expected by this scenario (Fig. 3, *lower right*). This conclusion is drawn largely irrespective of their distance. We show with a dotted line in Fig. 3, *lower right*, the $\sim 2.5 \times$ lower stellar mass that would be measured for the galaxies at a 13 Mpc distance (Trujillo et al. 2019) and would still have them within the scatter of the established relationships. A possible explanation is that they could instead be tidal dwarfs formed at higher redshift where gas is less enriched (see e.g. Fensch et al. 2019b, section 5.5). In this case, it would not be clear how these galaxies would survive the tidal field of the group until the present day due to their low dark matter content.

5.5 Tidally stripped stellar material

It has also been proposed that DF2 and DF4 may each be the remnants of a tidally stripped galaxy (Ogiya 2018; Montes et al. 2020; Nusser 2020; Jackson et al. 2021; Macciò et al. 2021; Moreno et al. 2022; Ogiya et al. 2022). Notably, if this is the case, there is no need for

the galaxies to be stripped at the same time (and thus they would not necessarily have similar stellar populations). Deep imaging from Müller et al. (2019) failed to find the low surface brightness features that may be expected, in this scenario, to be associated with each galaxy. The stellar ages for DF2/DF4/DF9 allow any such event to have occurred up to ~ 9 Gyr ago. Therefore, any tidal features associated with the galaxies formation may have dissipated beyond the detection limit of Müller et al. (2019). However, this does not exclude the galaxies from *currently* undergoing a tidal interaction, for which there is evidence (Montes et al. 2020; Keim et al. 2022).

In order to produce the currently observed large GC systems for DF2/DF4 (~ 19 each; Shen et al. 2021a), a tidal stripping scenario would require the progenitor to be unrealistically GC-rich (Ogiya et al. 2022). The subsequent stripping would be expected to leave a trail of stripped, intragroup GCs that are presently not observed in the group (Buzzo et al. 2023). It is difficult to envision a stripping scenario that removes large quantities of the stellar mass without removing some of the GC system. The only possibility for this formation hypothesis to be valid is that the progenitor had a GC system that was more compact than usual and hence more resistant to tidal stripping (see appendix B of Ogiya et al. 2022).

6 CONCLUSIONS

In this work, we have performed a stellar population analysis of Keck/KCWI data targeting the galaxy DF9 to investigate its formation history. We placed particular emphasis on comparing our stellar population results with those of the other nearby dwarf galaxies DF2 and DF4 around NGC 1052. Our main conclusions are as follows:

(i) We measure a recessional velocity $1680 \pm 10\,\mathrm{km\,s^{-1}}$ for DF9 which places the galaxy in the NGC 1052 group and corrects the erroneous listing of the galaxy as a high-redshift quasar.

(ii) We recover an age and metallicity for the nucleus of DF9 that are in agreement with those of the stellar body of the galaxy. The high luminosity of the nucleus suggests a total mass that is approximately seven times the average for a Milky Way GC. We therefore suggest that the nucleus of DF9 formed via a combination of GC mergers and/or *in situ* star formation.

The age and metallicity we recover for the stellar body of DF9 are within uncertainties of literature ages and metallicities for the galaxies DF2 and DF4 also in the NGC 1052 group. Using them, we investigate the following:

(i) The likelihood that the commonality of characteristics of DF2/DF4/DF9 could be the result of random chance. The metallicities of the three galaxies may be the result of all following the dwarf stellar mass–metallicity relation. Given their environment, it is difficult to be conclusive on the likelihood of their common age occurring randomly.

(ii) The recent proposal that these three galaxies may have formed as part of a 'bullet dwarf' collision. Their common ages and metallicities are as expected for this scenario. However, the radial velocity of DF9 does not fit with a geometrically linear interpretation of the remnant dwarf trail. DF9 is either not part of the trail or the correlation of projected galaxy velocities cannot be linear. Furthermore, differences between the metallicities of the GCs around DF2/DF4 and their stellar bodies require an explanation in the scenario as currently posed.

(iii) A more general case of these galaxies forming from H I tidal debris. Our conclusions are the same as those for the 'bullet dwarf'

collision. However, it is now more difficult to explain the anomalous GC systems of two galaxies in the trail, DF2/DF4, without the special star-forming conditions induced by a high-speed collision. Additionally, the GCs' lack of an elevated metallicity for their stellar masses is at odds with this scenario.

(iv) If these galaxies may have formed as the result of tidal stripping. Our intermediate age confirms that each interaction may have occurred sufficiently long ago to allow tidal features to dissipate below the surface brightness limits of current imaging.

ACKNOWLEDGEMENTS

DATA AVAILABILITY

The KCWI data presented are available via the Keck Observatory Archive 18 months after observations are taken.

REFERENCES

Buzzo M. L. et al., 2022, MNRAS, 517, 2231
Buzzo M. L., Forbes D. A., Brodie J. P., Janssens S. R., Couch W. J., Romanowsky A. J., Gannon J. S., 2023, MNRAS, 522, 595
Cappellari M., 2017, MNRAS, 466, 798
Danieli S., van Dokkum P., Conroy C., Abraham R., Romanowsky A. J., 2019, ApJ, 874, L12
Dutta Chowdhury D., van den Bosch F. C., van Dokkum P., 2020, ApJ, 903, 149
Emsellem E. et al., 2019, A&A, 625, A76
Fahrion K. et al., 2020, A&A, 634, A53
Fahrion K. et al., 2021, A&A, 650, A137
Fahrion K. et al., 2022, A&A, 667, A101
Fensch J. et al., 2019a, A&A, 625, A77
Fensch J. et al., 2019b, A&A, 628, A60
Fosbury R. A. E., Mebold U., Goss W. M., Dopita M. A., 1978, MNRAS, 183, 549
Gannon J. S., Forbes D. A., Romanowsky A. J., Ferré-Mateu A., Couch W. J., Brodie J. P., 2020, MNRAS, 495, 2582
Harris W. E., 1996, AJ, 112, 1487
Iodice E. et al., 2021, A&A, 652, L11
Jackson R. A. et al., 2021, MNRAS, 502, 1785
Karachentsev I. D., Karachentseva V. E., Suchkov A. A., Grebel E. K., 2000, A&AS, 145, 415
Keim M. A. et al., 2022, ApJ, 935, 160
Kroupa P., 2001, MNRAS, 322, 231
Lee J., Shin E.-j., Kim J.-h., 2021, ApJ, 917, L15
Macciò A. V., Prats D. H., Dixon K. L., Buck T., Waterval S., Arora N., Courteau S., Kang X., 2021, MNRAS, 501, 693
Montes M., Infante-Sainz R., Madrigal-Aguado A., Román J., Monelli M., Borlaff A. S., Trujillo I., 2020, ApJ, 904, 114
Moreno J. et al., 2022, Nat. Astron., 6, 496
Morrissey P. et al., 2018, ApJ, 864, 93
Müller O. et al., 2019, A&A, 624, L6
Nusser A., 2020, ApJ, 893, 66
Ogiya G., 2018, MNRAS, 480, L106
Ogiya G., van den Bosch F. C., Burkert A., 2022, MNRAS, 510, 2724
Panter B., Jimenez R., Heavens A. F., Charlot S., 2008, MNRAS, 391, 1117
Román J., Jones M. G., Montes M., Verdes-Montenegro L., Garrido J., Sánchez S., 2021a, A&A, 649, L14
Román J., Castilla A., Pascual-Granado J., 2021b, A&A, 656, A44
Ruiz-Lara T. et al., 2019, MNRAS, 486, 5670
Sales L. V., Navarro J. F., Peñafiel L., Peng E. W., Lim S., Hernquist L., 2020, MNRAS, 494, 1848
Sardone A., Pisano D. J., Burke-Spolaor S., Mascoop J. L., Pol N., 2019, ApJ, 871, L31
Shen Z., van Dokkum P., Danieli S., 2021a, ApJ, 909, 179
Shen Z. et al., 2021b, ApJ, 914, L12
Shin E.-j., Jung M., Kwon G., Kim J.-h., Lee J., Jo Y., Oh B. K., 2020, ApJ, 899, 25
Silk J., 2019, MNRAS, 488, L24
Simon J. D., 2019, ARA&A, 57, 375
Tollerud E., 2015, available at: https://gist.github.com/eteq/5000843
Trujillo-Gomez S., Kruijssen J. M. D., Keller B. W., Reina-Campos M., 2021, MNRAS, 506, 4841
Trujillo I. et al., 2019, MNRAS, 486, 1192
Trujillo I. et al., 2021, A&A, 654, A40
Vazdekis A. et al., 2015, MNRAS, 449, 1177
van Dokkum P. G., Abraham R., Merritt A., Zhang J., Geha M., Conroy C., 2015, ApJ, 798, L45
van Dokkum P. et al., 2018a, Nature, 555, 629
van Dokkum P. et al., 2018b, ApJ, 856, L30
van Dokkum P., Danieli S., Abraham R., Conroy C., Romanowsky A. J., 2019, ApJ, 874, L5
van Dokkum P. et al., 2022a, Nature, 605, 435 (vD + 22)
van Dokkum P. et al., 2022b, ApJ, 940, L9

This paper has been typeset from a TEX/LATEX file prepared by the author.